NANO LETTERS

2002
Vol. 2, No. 10
1149−1155

Nanostructured Polyethylene-POSS Copolymers: Control of Crystallization and Aggregation

A. J. Waddon,* L. Zheng, R. J. Farris, and E. Bryan Coughlin*,‡

Department of Polymer Science and Engineering, University of Massachusetts, Amherst Massachusetts 01003

Received June 18, 2002; Revised Manuscript Received August 5, 2002

ABSTRACT

Nanoscale structure formation in copolymers of polyethylene (PE) and polyhedral oligomeric silsesquioxane (POSS) with norbornene and cyclopentyl side-groups can be controlled through choice of crystallization conditions. Aggregates of both crystalline PE and crystalline POSS are found when crystallized from the melt. A self-assembled, two-phase crystalline structure, consisting of POSS crystalline domains molecularly connected to PE crystalline domains, is formed. Constraints on domain growth arise from molecular architecture, likely leading to anisotropy in the shape of POSS domains. Considerable suppression of POSS crystallization is found on precipitation from solution. The origin of the frustration of crystal growth and the introduction of disorder is discussed. Structural investigative methods include X-ray diffraction and transmission electron microscopy. Degradation temperatures are found to be dependent on the morphology of the nanocomposites, with possible implications for improved thermal resistance.

Introduction. Copolymers containing inorganic polyhedral oligomeric silsesquioxane (POSS)[1] side-group substituents represent a novel category of nanoscale structured materials. These are attracting enormous interest as candidate materials for high-temperature and fire-resistance applications.[2] This stems from the significant enhancement of thermal and mechanical properties compared to the unsubstituted polymer. These superior properties are directly related to the nanoscale structure of the materials. The general molecular structure of an individual unit of POSS is shown in Figure 1a. This consists of Si_8O_{12} arranged in a cage-like structure. A variety of substituents can be attached at the eight corner positions around the cage. Typically, seven of these are occupied by identical groups (R in Figure 1a), which control the degree of compatibility of the POSS with the host polymer, while the remaining position is occupied by a reactive group (X in Figure 1a), which provides the site for incorporation into a copolymer. A variety of POSS-containing copolymers have been synthesized in this manner.[3−15] Nevertheless, despite the appreciable interest in the synthesis and engineering properties of the copolymers, their physical structure is still largely unexplored. This paper directly addresses this issue.

In principle, POSS units can be dispersed throughout the material as isolated nanoparticles or as aggregates of POSS units. Indeed, although different authors have attributed enhancement of properties to both dispersion[8,16] and aggregation of POSS,[9,11] there is very little work that deals directly with the physical character of the material. POSS units themselves are crystallizable in the form of the unpolymerized monomer;[17−21] they can also form crystalline domains when covalently linked to a polymer backbone as pendant groups.[6,8−11,15,22,23] However, in this case, crystal growth will be constrained in at least one dimension by the presence of the macromolecule. This is likely to lead to the growth of anisotropic domains, with at least one dimension on the scale of a few nanometers.[23]

The extent of possible POSS crystallization depends not only on the amount of POSS incorporated into the polymer chain but also on the nature of the host chain. Many reported POSS copolymers have been based on polymers that are themselves inherently uncrystallizable.[6,8,10] Previously we reported some of the first structural work on systems based on crystallizable host polymers, specifically polyethylene (PE).[23] It was found that melt crystallized PE−POSS nanocomposites can contain domains of both crystalline PE and crystalline POSS, as well as a significant amorphous component. In the present contribution we now show that the degree of POSS crystallization and final self-assembled nanostructure are also highly dependent on thermal history and, furthermore, that these can be controlled and tailored by judicious selection of processing conditions. Specifically, we compare crystallization from solution with crystallization from the melt and show how processing conditions either promote or inhibit the formation of aggregates of POSS

* Corresponding authors.
‡ Couglin@mail.pse.vmass.edu

10.1021/nl020208d CCC: $22.00
Published on Web 09/06/2002

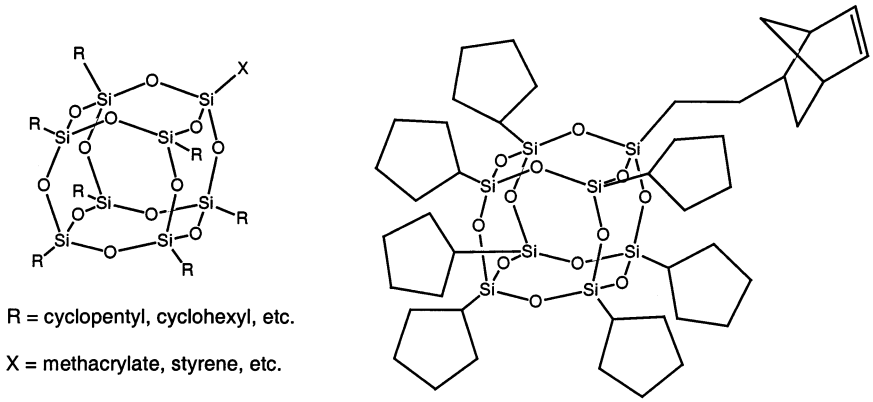

Figure 1. (a) Generalized structure of single POSS monomer unit[23], (b) specific structure of norbornene-cyclopentyl POSS used in this study.

Table 1: Molecular Characterization of PE-*co*-POSS Copolymers[a]

sample	POSS in copolymers (wt %)	POSS in copolymers (mol %)	M_w ($\times 10^3$ g/mol)	polydispersity index
PE	0	0	328	1.26
PE−POSS1	19	0.64	315	1.43
PE−POSS2	27	1.0	315	1.67
PE−POSS3	37	1.6	516	1.73
PE−POSS4	56	3.4	446	2.07

[a] Gel permeation chromatography was performed using a Polymer Laboratories high-temperature GPC PL-220 equipped with a Wyatt high-temperature light scattering detector miniDAWN (HTmD) at 135 °C in trichlorobenze. The miniDAWN detector contains a 690 nm diode laser. We used values of −0.104 for the d*n*/d*c* of polyethylene.

nanocrystals. The nanoscale structure is demonstrated to radically change the physical nature and thermal degradation behavior of the final material.

Materials. A cyclopentyl-POSS-norbornenyl monomer 1-[2-5-norbornen-2-ylethyl]-3,5,7,9,11,13,15-heptacyclopentylpentacyclo [9.5.1.1^{3,9}.1^{5,15}.1^{7,13}] octasiloxane, containing seven cyclopentyl and one norbornenyl group at the corner positions, was obtained from Phillips Laboratory, Propulsion Directorate, Edward's AFB. The specific structure of this particular monomer is shown in Figure 1b. The monomer starts to decompose or sublime with onset temperatures of ∼300 and 220 °C in nitrogen and air, respectively. No melting was detected below these temperatures with standard differential calorimetry procedures. The norbornenyl group was used as the reactive site to incorporate POSS as side units on a PE host polymer, as described in ref 24 using a metallocene catalyzed reaction. "As-synthesized" materials were recovered after synthesis by precipitation in methanol at room temperature. A series of POSS−PE copolymers of varying POSS contents were prepared in this manner. The exact mole fractions and weight fractions of POSS are shown in Table 1. It should be noted that, although the mole fractions are relatively low, the weight fractions are considerably higher (a consequence of the high molecular weight of the POSS unit). ^{1}H and ^{13}C NMR characterization indicated no significant residual POSS monomer content in these copolymers. Unfortunately, information regarding precise sequence distribution is not available. For comparison, we also conducted structural studies on both PE homopolymer and on the unpolymerized cyclopentyl-POSS-norbornene monomer material. However, because of low reactivity, it was not possible to synthesize the homopolymer of POSS.

Experimental Section. *POSS−PE Copolymers and PE Homopolymer.* Solution Crystallization. As-synthesized copolymers and PE homopolymer were dissolved in hot xylene to form solutions of 0.2% (wt/vol) and subsequently cooled to room temperature. Only slight precipitation of copolymers occurred on cooling, the amount of precipitation increasing with increasing PE content. Full precipitation was induced by the addition of acetone. The precipitates were dried to form films for examination by wide-angle X-ray diffraction (WAXD). Specimens were also prepared for transmission electron microscopy (TEM) by drying the suspensions of precipitates directly on carbon-coated TEM grids.

Melt Crystallization. As-synthesized copolymers and homo PE were compression molded at 180 °C for 10 min and cooled to room temperature, as previously described.[23] The melting temperatures of polyethylene in these copolymers are in the range of 100−130 °C.

POSS Monomer. Solution Crystallization. POSS monomer was found to be readily soluble in xylene, even at room temperature. In marked contrast to the POSS-containing copolymers, this failed to precipitate from xylene solution on addition of acetone. Specimens for TEM were therefore prepared by depositing the xylene solution directly on carbon-coated grids and allowing the solvent to evaporate.

Methods of Investigation. The crystalline nature of both solution and melt crystallized materials were characterized by X-ray diffractometry using a Siemens D500 diffractometer operating in normal-transmission mode with Ni filtered CuKα radiation.

Solution crystallized materials on carbon-coated TEM grids were obliquely shadowed with gold. In some cases calibration polystyrene latex spheres of 0.87 μm were also

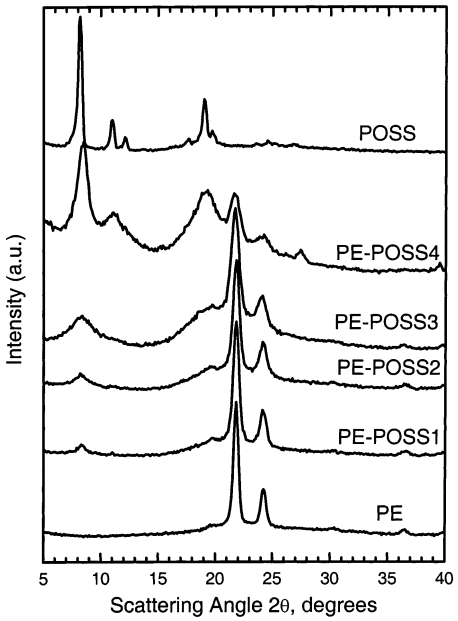

Figure 2. Diffractograms of "as-synthesized" PE−POSS copolymers, "as-synthesized" PE homopolymer, and "as-received" POSS monomer.

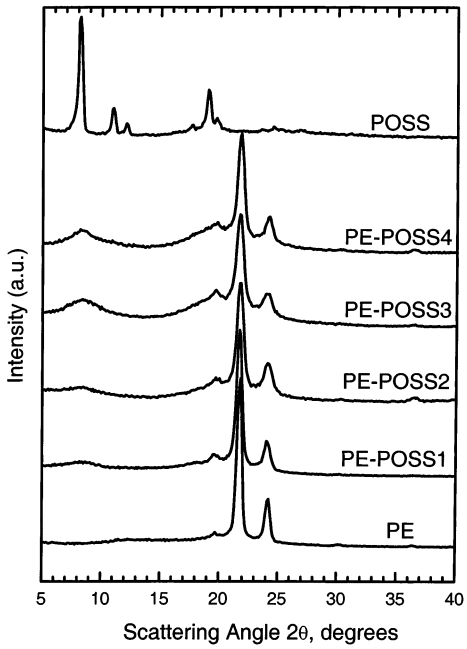

Figure 3. Diffractograms of PE−POSS copolymers and PE homopolymer; precipitated from xylene solution by addition of nonsolvent. (Trace from "as-received" POSS monomer also shown.)

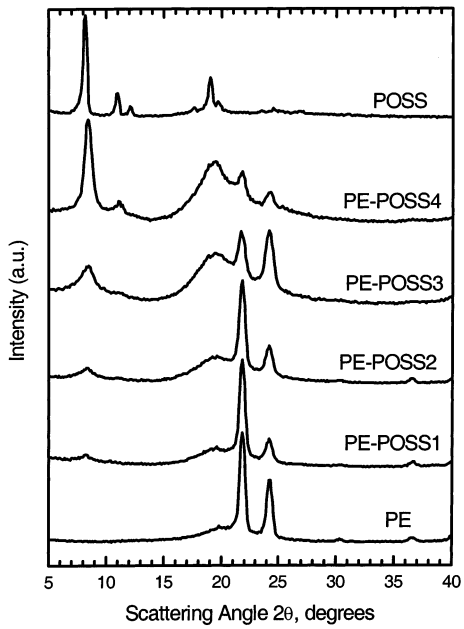

Figure 4. Diffractograms of PE−POSS copolymers and PE homopolymer; crystallized by cooling from the melt at 180 °C. (Trace from "as-received" POSS monomer also shown.)

deposited on grids prior to shadowing. Grids were examined in a JEOL 100CX TEM, operating at an accelerating voltage of 100 kV.

Thermogravimetric analysis was carried out using a TA Instruments TGA 2050 thermogravimetric analyzer with a heating rate of 20 °C/min from room temperature to 700 °C under a continuous air purge of 50 mL/min.

Results. The diffractograms of the initial as-synthesized copolymers are shown in Figure 2. For comparison, results from as-synthesized homo PE and as-received POSS monomer are also shown. It is apparent that the traces from the copolymers show crystalline features characteristic of both PE homopolymer and POSS monomer: (a) crystalline PE peaks at 21.6° (equivalent to an interplanar spacing of 0.411 nm), 24.1° (0.37 nm), and 36.5° (0.25 nm), corresponding to 110_{PE}, 200_{PE}, and 020_{PE}, respectively. These peaks broaden in the copolymers compared to homo PE. (b) crystalline POSS peaks at ∼8.2° (1.08 nm), evident in all copolymers, and at 11.0° (0.8 nm), evident in the material of highest POSS content. Both these signals can be unambiguously identified as originating from crystalline POSS. Although the peak at ∼19.7° (0.45 nm) is close to the expected position for the 010 of the PE monoclinic modification, it also corresponds to the position of a major POSS signal, and, because this intensifies with POSS content, it is considered that this is probably a contribution from crystalline POSS.

The corresponding diffractograms for the materials precipitated from solution are shown in Figure 3. For ease of comparison, the diffractogram from the as-received POSS monomer is also reproduced here and in Figure 4. It is immediately apparent that all the copolymer traces are significantly different from those of the as-synthesized materials in that they are dominated by the PE crystalline component with weaker and significantly broadened POSS peaks. On inspection it is also apparent that the PE reflections in the copolymers are broader in comparison to the homo PE.

These results also contrast strikingly with the diffractometer traces for the melt crystallized materials of the same copolymers, Figure 4. Here it is seen that the contribution from crystalline POSS is far stronger and that, for the material with highest POSS content, the POSS reflections dominate and PE reflections appear very broad and very weak.

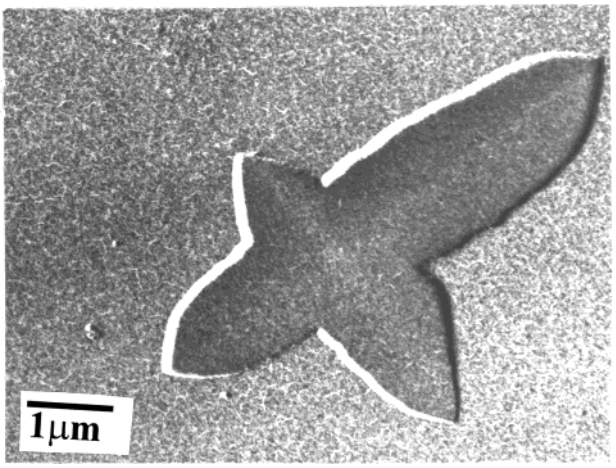

Figure 5. Transmission electron micrograph (bright-field) of crystal of POSS monomer precipitated from xylene solution by evaporation of solvent. Gold shadowed.

More information regarding the underlying microstructure in the xylene crystallized materials is obtained by direct morphological examination using TEM. Figure 5 shows a micrograph of the POSS monomer precipitated from xylene. This is dominated by well-formed crystals a few micrometers in length and, from shadow length measurement, a few tens of nanometers in thickness. The abundance of reentrant corners, which leads to a "star" shape, is suggestive of crystal twinning, although this is not an issue further developed here. Electron diffraction patterns consisting of spots were obtained and obviously emanate from single crystals. A variety of patterns, corresponding to projections along different crystallographic axes, were found. Importantly, the observed spacings were consistent with values previously found with X-ray diffraction, confirming the identification of the crystals as POSS.

Figure 6 shows an electron micrograph of the PE homopolymer (Figure 6a) and electron micrographs of the copolymers (Figure 6 b−e), crystallized from xylene in all cases. In contrast to Figure 5 above, an abundance of aggregates of small crystals is observed. Moreover, with increasing POSS content, the morphology of the crystals becomes more poorly defined. Crucially, electron diffraction typically comprised *hk*0 reflections from the PE lattice, identifying the aggregates as PE crystallites, oriented with the chain axis parallel to the electron beam (and hence parallel to the thin dimension of the crystal).

Separate POSS crystals are difficult to identify with any certainty in these micrographs. Also, complimentary direct microscopy evidence on the melt crystallized series was not readily available due to the inherent difficulties in preparing thin sections. However, apparent POSS crystal sizes can be estimated indirectly from the relative broadening of the main POSS X-ray diffraction peak at $2\theta = 8.2°$ using the Scherrer equation ($L = \lambda/(\beta \cos \theta)$, where L is the apparent crystal size, λ is the X-ray wavelength, and β is the full width at half-maximum (fwhm) of the peak. Table 2 shows estimates of L estimated from values of β for this reflection (used without correction for instrumental broadening) for samples in which β could be reasonably estimated. Of course, broadening can also be caused by crystal disorder effects which may also be significant here; furthermore, a highly anisotropic crystal will show different values of β depending on which reflecting crystallographic plane is used in the calculation. This makes the estimation of absolute crystal sizes from the Scherrer equation inherently unreliable, and values of L should rather be considered as "apparent crystal sizes". The apparent crystal size calculated for the monomer is much lower than lateral size indicated by microscopy (Figure 5) but is of the same order as the crystal thickness estimated from shadow lengths. Table 2 also shows that apparent crystal sizes in the copolymers are smaller than in the monomer, that they decrease with decreasing POSS content, and are significantly larger in the melt crystallized series than in the solution crystallized series.

Table 2: Apparent Crystal Sizes, L, of POSS Crystals Estimated from the fwhm of the X-ray Reflection at $2\theta = 8.2°$ Using the Scherrer Equation

	L, nm	
sample	solution crystallized	melt crystallized
PE−POSS3	3	7
PE−POSS4	5	11
POSS monomer	22	

Discussion. Clearly different crystallization procedures can produce dramatic differences in final copolymer structure. For both solution and melt crystallization the starting materials were the as-synthesized materials, precipitated from methanol. From WAXD the as-synthesized materials showed crystalline populations of both PE and POSS at all levels of loading. However, subsequent thermal treatment is seen to radically modify the crystalline structure.

On precipitation from xylene, crystallization of PE dominates with only a very minor degree of POSS crystallization. The reasons for this lie in the details of the crystallization procedure. The PE component will unquestionably dissolve in xylene at high temperature. Moreover, the ready solubility of the POSS monomer in xylene at room temperature suggests that POSS crystals in the as-synthesized copolymers will also be soluble under these conditions. On addition of nonsolvent, the propensity for precipitation of the copolymers increases with increasing PE content (POSS monomer failing to precipitate at all), suggesting that the precipitation is due to crystallization of the PE component. This will therefore lay down a "scaffold" of PE around which POSS must be accommodated. Consequently, during subsequent drying, the POSS component can only crystallize in the confined spatial environment between preexisting PE crystals. POSS crystallization is therefore subject to a purely geometric constraint provided by the spatial limitations around PE crystals. Second, there is also a topological constraint arising from the molecular connectivity between the two components. Because POSS units are present as side units on polymeric chains rather than as free units, POSS crystal development is likely to be frustrated by the physical presence of the attached macromolecule. Third, any prior crystallization of PE will effectively "pin" chains into PE crystals, providing

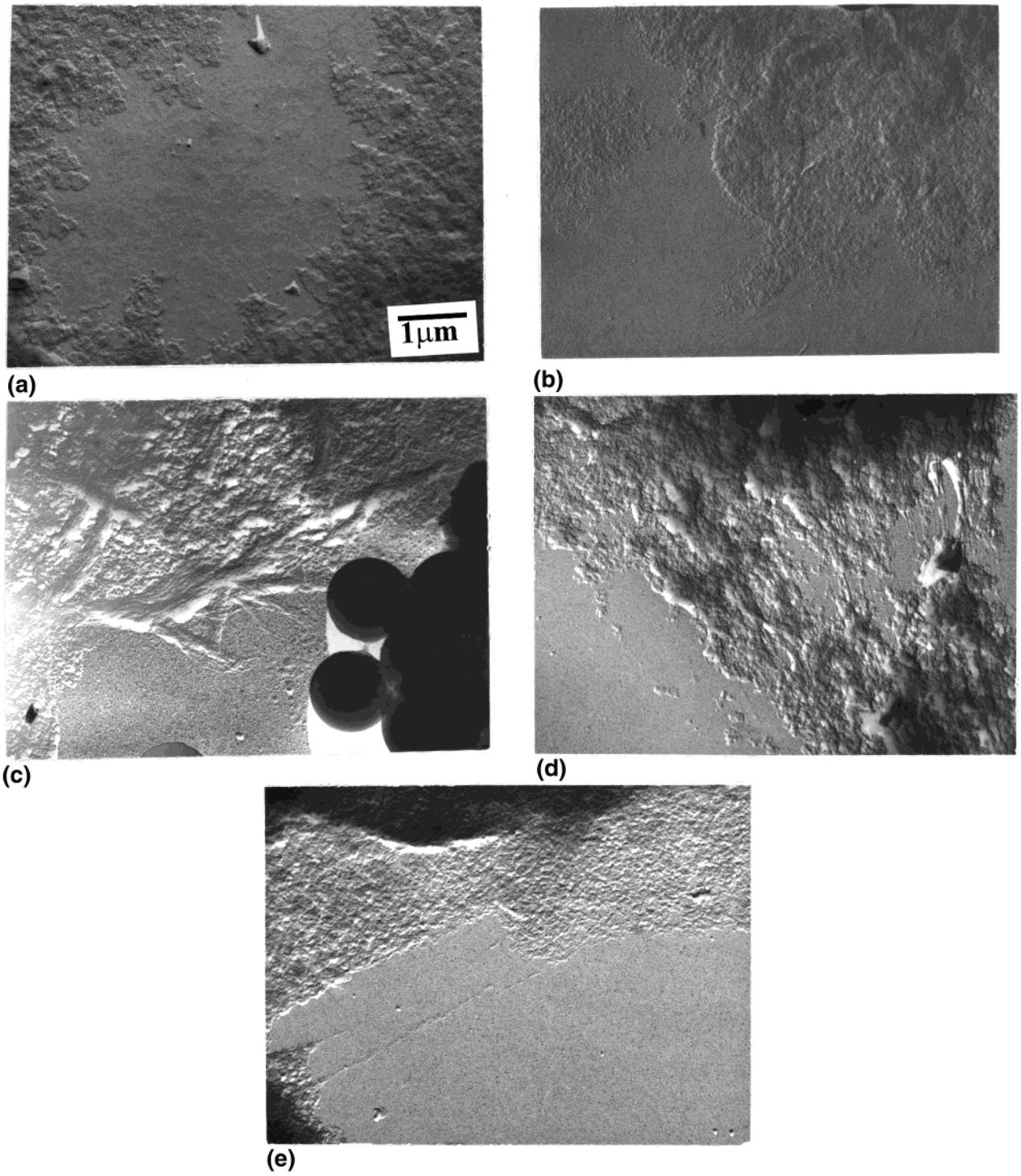

Figure 6. Transmission electron micrographs of homo PE (a) and PE−POSS copolymers with following wt % of POSS: (b) 19%, (c) 27%, (d) 37%, and (e) 56%), precipitated from xylene solution by addition of nonsolvent. Gold shadowed.

a further topological constraint on the ability of the POSS to adopt favorable conformations for crystallization. These constraints serve to limit POSS crystallization and lead to a structure dominated by crystalline PE within which POSS must exist as a disordered component, very probably mainly dispersed as unassociated POSS units throughout the polymer matrix.

It is also apparent from considerations of PE X-ray line broadening and TEM that the PE forms increasingly smaller and ill-defined crystals with increasing POSS content, suggesting that the PE crystals are themselves subject to frustrated growth. The obvious inference is that this is a result of disruption of the lattice due to the attachment of POSS units to the chain which, at a diameter of ∼1.5 nm, are far too large to be included within the lattice. Exclusion of these units then disrupts the usual, relatively regular, development of PE crystals.

Turning to the melt crystallized materials, the melting point defined for this series of copolymers is in fact the melting point of the PE lattice (100−130 °C).[24] The maximum

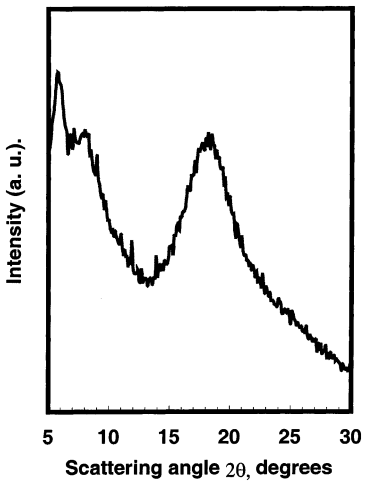

Figure 7. Diffractogram of PE−POSS copolymer (POSS4) with 56 wt % POSS, taken at 180 °C. The sample was initially crystallized by cooling from the melt to room temperature; it was then reheated to 180 °C, at which temperature the diffractometry was performed. (The peak at ∼6° is from Kapton windows in the heating cell.)

temperature reached during melt processing (180 °C) is clearly sufficient to melt the PE. Figure 7 shows a diffractometer trace at ∼180 °C of the copolymer (POSS4) with highest POSS content (56 wt. %). The well-defined peak at ∼6° is from Kapton used in the heating cell and can be disregarded. The sharp crystalline PE reflections have, of course, been replaced with an amorphous halo centered around ∼18°. However, now the main POSS signal at 8.2° also appears as a weakened and broadened signal suggestive of noncrystalline domains of POSS. This implies that the melting point of the POSS is very significantly reduced in the copolymer compared to the monomer state. The point at which POSS domains lose crystallinity on heating and when they recrystallize on cooling is the subject of our current attention, but whether recrystallization occurs before or after crystallization of the PE component, the PE must necessarily crystallize within the confined space between preexisting POSS domains, eventually leading to self-assembly of two distinct, but molecularly connected, crystalline phases. This is clearly the opposite of the former situation described above and, in this case, crystallization of PE will be subject to similar geometric and topological constraints. The severity of the constraints imposed by the preexisting POSS domains increases with POSS content in the copolymer. Accordingly, the final self-assembled structure consists of POSS crystals plus a relatively disordered PE crystal component. It should, however, be noted that, regardless of processing conditions, in copolymers POSS crystals will always be subject to the constraints imposed by the physical attachment to the macromolecule (described above) which is likely to frustrate three-dimensional crystal development.

In summary, it is clear that two distinctly different crystallizing components are present in these copolymers and that the final structure depends on their respective crystallization kinetics under different crystallization conditions. In the extreme, either component can be forced to form a scaffold around which the other must be accommodated. Prior existence of domains of one component frustrates the crystallization of the second. By careful choice of processing conditions it is therefore possible to produce radically different physical structures from the same copolymer. The self-assembled structure with two crystalline phases in nonblock copolymers is, to our knowledge, unique. We are not aware of other examples in which pendant groups are rejected from the macromolecule lattice to form a second, separate nanoscale crystal. This situation is distinct from the well studied nanoscale structures formed from block copolymers which rely on incompatibility between different blocks in the main chain.

The dramatic differences in structures in the POSS−PE system are, of course, expected to have significant consequences for properties. We take this opportunity to briefly illustrate this using, as an example, the different responses in thermal gravimetric analysis (TGA) for xylene crystallized and melt crystallized materials, Figure 8a and Figure 8b, respectively. The melt crystallized copolymers have far

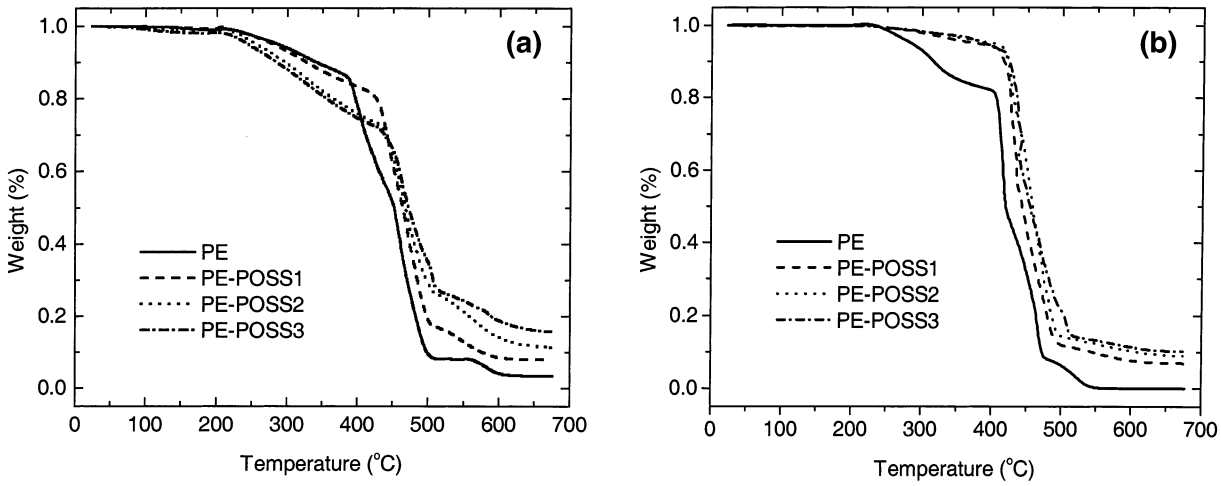

Figure 8. Thermal gravimetric analysis (TGA) of PE−POSS copolymers and PE homopolymer crystallized (a) from solution in xylene by the addition of nonsolvent and (b) from the melt. In the case of (a) the copolymers showed significant suppression of POSS crystallization, while in (b) the copolymers showed significant crystallization of POSS.

superior thermal resistance (and presumably also fire resistance) than are seen for the xylene crystallized materials. In the melt crystallized case, significant weight loss (90% original weight retention) is observed above 400 °C (Figure 8b), while in the xylene crystallized case, the same weight loss occurs in the range ~230−330 °C (Figure 8a). Moreover, the melt crystallized copolymers show less variability in TGA than their xylene crystallized counterparts. Interestingly, the 90% weight retention temperature increases with POSS content for the melt crystallized series but decreases with POSS content for the xylene crystallized series. Structurally, the melt crystallized materials contain significant levels of both POSS and PE crystallinity, while the solution crystallized materials have structures dominated by PE crystals with very few crystalline aggregates of POSS. Thermal decomposition of polymers is a complicated process and we recognize that many factors can affect this. It is however, reasonable to suggest that the development of larger domains of POSS may possibly confer the improvement in thermal stability to the entire material. It is also possible that differences in nanostructured morphology result in differences in thermal conductivities which, in turn, lead to differences in thermal decomposition behavior. The details of the mechanism by which the morphology influences thermal degradation remain to be fully elucidated, however. Further investigations correlating nanostructure with properties are being conducted in this ongoing research program.

Conclusions. Copolymers of PE and POSS in which POSS units are incorporated as substituent side units on the polymer chain can form separate populations of crystalline PE and crystalline POSS. These crystal domains must necessarily be connected on the molecular level to form a self-assembled nanoscale structure. Furthermore, this can be modified and tailored by control of processing conditions. The structure can be forced to develop around a preexisting nanoscale scaffold formed by domains of a selected component (either PE or POSS). The macroscopic molten state consists of disordered domains of POSS in an environment of molten PE; the POSS domains then form the nanoscaffold for subsequent crystallization of PE on cooling. In contrast, although dissolution in xylene removes both crystalline components, on subsequent precipitation, the PE component crystallizes preferentially and therefore forms the nanoscaffold for later crystallization of POSS. In both cases, the molecular connectivity between the POSS and PE provides a source of constraint and frustration for crystallization, and indeed, crystallization of POSS can be significantly suppressed. It is also apparent that the details of the nanoscale structure have important consequences for thermal properties, with an increase in thermal degradation resistance observed if there is significant crystallization of POSS.

Acknowledgment. The authors acknowledge the support of the NSF funded MRSEC at the University of Massachusetts, Amherst.

References

(1) POSS is a registered trademark of Hybrid Plastics www.hybridplastics.com.
(2) Mantz, R. A.; Jones, P. F.; Chaffee, K. P.; Lichtenhan, J. D.; Gilman, J. W.; Ismail, I. M. K.; Burmeister, M. J. *Chem. Mater*. **1996**, *8*, 1250.
(3) Lichtenhan, J. D. In *Polymeric Materials Encyclopedia*; Salamone, J. C., Ed.; CRC Press: Boca Raton, 1996; p 7768.
(4) Schwab, J. J.; Lichtenhan, J. D. *Appl. Organomet. Chem.* **1998**, *12*, 707.
(5) Lichtenhan, J. D.; Vu, N. Q.; Carter, J. A.; Gilman, J. W.; Feher, F. J. *Macromolecules* **1993**, *26*, 2141.
(6) Lichtenhan, J. D.; Otonari, Y. A.; Carr, M. J. *Macromolecules* **1995**, *28*, 8435.
(7) Haddad, T. S.; Lichtenhan, J. D. *Macromolecules* **1996**, *29*, 7302.
(8) Lee, A.; Lichtenhan, J. D. *Macromolecules* **1998**, *31*, 4970.
(9) Romo-Uribe, A.; Mather, P. T.; Haddad, T. S.; Lichtenhan, J. D. *J. Polym. Sci., Part B: Polym. Phys.* **1998**, *36*, 1857.
(10) Lee, A.; Lichtenhan, J. D. *J. Appl. Polym. Sci.* **1999**, *73*, 1993.
(11) Mather, P. T.; Jeon, H. G.; Romo-Uribe, A.; Haddad, T. S.; Lichtenhan, J. D. *Macromolecules* **1999**, *32*, 1194.
(12) Shockey, E. G.; Bolf, A. G.; Jones, P. F.; Schwab, J. J.; Chaffee, K. P.; Haddad, T. S.; Lichtenhan, J. D. *Appl. Organomet. Chem.* **1999**, *13*, 311.
(13) Fu, B. X.; Zhang, W. H.; Hsiao, B. S.; Rafailovich, M.; Sokolov, J.; Johansson, G.; Sauer, B. B.; Phillips, S.; Balnski, R. *High Perform. Polym.* **2000**, *12*, 565.
(14) Hsiao, B. S.; White, H.; Rafailovich, M.; Mather, P. T.; Jeon, H. G.; Phillips, S.; Lichtenhan, J.; Schwab, J. *Polymer* **2000**, *49*, 437.
(15) Fu, B. X.; Hsiao, B. S.; Pagola, S.; Stephens, P.; White, H.; Rafailovich, M.; Sokolov, J.; Mather, P. T.; Jeon, H. G.; Phillips, S.; Lichtenhan, J.; Schwab, J. *Polymer* **2001**, *42*, 599.
(16) Bharadwaj, R. K.; Berry, R. J.; Farmer, B. L. *Polymer* **2000**, *41*, 7209.
(17) Barry, A. J.; Daudt, W. H.; Domicone, J. J.; Gilkey, J. W. *J. Am. Chem. Soc.* **1955**, *77*, 4248.
(18) Larsson, K. *Ark. Kemi* **1960**, *16*, 203.
(19) Larsson, K. *Ark. Kemi* **1960**, *16*, 209.
(20) Larsson, K. *Ark. Kemi* **1960**, *16*, 215.
(21) Auf der Heyde, T. P. E.; Burgi, H.-B.; Burgy, H.; Tornroos, K. W. *Chimia* **1991**, *45*, 38.
(22) Mather, P. T.; Chun, S. B.; Pyun, J.; Matyjaszewski, K. *Polym. Prepr. (Am. Chem. Soc., Div. Polym. Chem.)* **2000**, *41*(1), 582.
(23) Zheng, L.; Waddon, A. J.; Farris, R. J.; Coughlin, E. B. *Macromolecules* **2002**, *35*, 2375.
(24) Zheng, L.; Farris, R. J.; Coughlin, E. B. *Macromolecules* **2001**, *34*, 8034.

NL020208D